

CASCADING TRANSFORMER FAILURE PROBABILITY MODEL UNDER GEOMAGNETIC DISTURBANCES

Pratishtha Shukla
James Nutaro
Srikanth Yoginath

Oak Ridge National Laboratory
One Bethel Valley Road
Oak Ridge, TN, 37830, USA

ABSTRACT

This paper develops a probabilistic model to assess the cascading failure of transformers in an electric power grid experiencing geomagnetic disturbances caused by a solar storm. We propose a model in which the probability of failure is a function of the intensity of the solar storm, the physical properties of the transformer, the geographical location of the transformer, and the flow of electrical power. We demonstrate the proposed model using the IEEE 14-bus system and several notional solar storms. The model quickly computes the initial and cascading failure probabilities of the transformers in the system as a first step towards quantifying the risks posed by future solar storms.

1 INTRODUCTION

Solar radiation storms occur when a large-scale magnetic eruption, often causing a coronal mass ejection (CME) and associated solar flare, accelerates charged particles in the solar atmosphere to very high velocities. When this solar material strikes Earth's magnetic environment, that is, the magnetosphere, it sometimes creates geomagnetic disturbances (GMDs). The impacts of these GMDs can range from mild to extreme, but in a world increasingly dependent on technology, their effects are growing ever more disruptive.

For example, a destructive solar storm in 1989 caused electrical blackouts across Quebec for 12 hours, plunging millions of Canadians into the dark and closing schools and businesses (Boteler 2019). Of particular concern is damage to the enormous transformers that connect generators and loads to the high-voltage transmission system. Damage to these transformers could produce long-lasting blackouts when spares are not readily available (National Research Council 2009; Kappenman 2012).

A study by Lloyd's and Atmospheric and Environmental Research, Inc. estimated that extreme solar events might occur every 150 years on average (Lloyd's 2013). The last such storm was the Carrington event in 1859 which, if it were to happen today, could cause damages exceeding a trillion dollars and outages lasting from months to years (Lloyd's 2013; National Research Council 2009; Kappenman 2012). A 2019 study by (Hayakawa et al. 2019) suggests such events may be even more frequent, concluding that "while this event has been considered to be a once-in-a-century catastrophe, the historical observations warn us that this may be something that occurs more frequently and hence might be a more imminent threat to modern civilization."

Effective preparation for a solar storm depends on timely warning of its potential impact on an electric power system. In extreme cases, preparation may entail shutting down parts of the electric power system that are at high risk. However, the loss of electricity involves commensurate economic losses, making such preparations unattractive unless the perceived risk is very high. Therefore, accurate and timely risk projections can be important in emergency preparedness.

We take a step towards providing risk projections by examining some of the main components of a model to estimate the risk of initial and cascading transformer failures in an electrical power system during a solar storm. Our initial model has three components. The first is a probabilistic model of transformer failure as a function of load and induced currents. The second is a power flow model to estimate the loading of transformers. The third is a model for currents induced by a solar storm as a function of storm intensity and the latitude and relative orientation of the transformer.

With this model, we demonstrate a method of analysis that proceeds from the expected storm intensity and a pre-storm power flow to calculate the probabilities of subsequent loss scenarios. When combined with the economic damages associated with a failure scenario, these probabilities could form the basis of a quantitative risk assessment to guide preparations for the storm. Our main contribution lies in developing this probabilistic model for cascading failures of transformers during a solar storm.

The proposed model takes a first step toward the possibility of a real-time tool for conducting risk assessments to complement space weather forecasts, such as those provided in the United States by the Space Weather Prediction Center within the National Oceanic and Atmospheric Administration (NOAA). We envision the proposed model, when fully developed, as a natural complement to analysis tools, such as the North American Energy Resilience Model (NAERM) (Department of Energy 2019), that provide situational awareness and risk-related analyses for power system operators and other stakeholders.

The rest of the paper is organized as follows. We briefly describe geomagnetically induced currents (GIC) and their computation in Section 2. The proposed probability model is presented in Section 3 followed by a simulation case study of the IEEE 14-bus system conducted in Section 4. Section 5 concludes the paper.

2 SOLAR STORMS AND TRANSFORMERS

A transformer consists of three main components: the primary winding, which acts as an input; the second coil, the secondary winding, which acts as the output, and the iron core, which strengthens the magnetic field connecting the pair of windings. A transformer has no internal moving parts and transfers energy from one circuit to another by electromagnetic induction. The flux and induced current in the transformer windings heat the core resulting in a temperature rise. This temperature increase is controlled by cooling devices to avoid the explosive effects of a highly overheated core.

Cooling of the transformer may involve heat exchangers, radiators, fans, oil pumps, or some combination of these. These devices can handle typical temperature rises caused by power surges that may occur during network outages. However, the design of the cooling devices does not necessarily account for the possibility of very high current surges in the transformer. Such surges have been experienced due to solar storms such as the Quebec magnetic storm of 1989 (Boteler 2019).

Models focusing on the impacts of high-intensity solar storms on transformers are sparse (Ramírez-Niño et al. 2016). Most of these models focus on short-term effects such as current harmonics, an increase in reactive power demand, and so forth. Of the few looking into the heating of transformers, focus on the impact on the physical aspects, such as the heating of tank oil and the temperature rise of the core (Dehghanian et al. 2019). However, none consider probability modeling, the cascading effects of failing power transformers, or their consequent impacts on the electric grid's reliability. To the best of our knowledge, the proposed model is the first to assess cascading transformer failures under GMDs.

2.1 Geomagnetically Induced Currents

GMDs give rise to geomagnetically induced currents (GICs) that enter the power grid through grounded transformer neutrals, flow through the windings, circulate through the transmission lines, and finally flow through another grounded transformer to leave the grid. They are quasi-Direct Currents (Q-DC) that are a function of ground conductivity, orientation, and the intensity of the geomagnetic field.

GICs may affect the power grid in many ways, of which the most prominent is their effects on transformers, specifically the ones that are a part of the transmission system. Ground transmission networks with high voltage levels are the most susceptible to GICs because the separation between grounded transformers is enough for GICs to reach levels of hundreds of Amperes in a neutral conductor. In particular, GICs in transformers may increase reactive power losses leading to voltage collapse, and the harmonic content in currents causes false tripping of relay protection devices. However, these are short-term effects that the system recovers from after the solar storm has passed.

More severe GICs may cause the melting of metallic components by hot-spot heating, damaging the transformers or even blowing up these components, leading to disabled transformers. This may result in blackouts for an extended period and require expensive and time-consuming repairs. Thus, GIC calculations are a vital part of assessing the risk that solar storms pose to the power grid because the high-intensity currents can disrupt the transmission structure easily through the transformers.

The inclusion of the impact of GICs in the power flow was first described by (Albertson et al. 1981). We use the method for power flow modeling with geomagnetic disturbances proposed by (Overbye et al. 2012) to compute the currents flowing in transformers situated at different geographical locations. Of the risks associated with geomagnetically induced currents, as noted in (Force, NERC Geomagnetic Disturbance Task 2012), the focus of (Overbye et al. 2012) is on the loss of reactive power support leading to the potential for a voltage collapse. However, this paper focuses on the risk of damage to high-voltage transformers and the propagation of risk to other transformers during a solar storm.

GICs are determined by solving a DC network of the form

$$\mathbf{I} = \mathbf{G}\mathbf{V} \quad (1)$$

where \mathbf{G} is a square matrix consisting of only real conductance values that include substation (or bus) grounding resistance values and the winding resistance values of transformers in the system. The vector \mathbf{V} contains entries for the bus DC voltages, and Norton equivalent currents are represented by \mathbf{I} .

To compute \mathbf{V} in our model, we follow a straightforward approach as in (Boteler and Pirjola 1998; Overbye et al. 2012). First, we begin with computing the induced voltages in the components of the electric grid due to the electric field generated by the solar storm. To calculate the GMD-induced line voltage, the electric field is integrated over the length of the transmission line. Hence, the DC voltage is calculated as

$$V = E_x L_x + E_y L_y \quad (2)$$

where $E_x = E \cos(\theta)$ is the electric field in the east-west direction (V/km), $E_y = E \sin(\theta)$ is the electric field in North-south direction (V/km), L_x is the eastward distance (km), L_y is the northward distance (km), and θ is the direction of the electric field E . A constant or uniform electric field is recommended for planning studies (Force, NERC Geomagnetic Disturbance Task 2012), which is independent of the transmission line's path. Therefore, information on the geographical location of the line's terminal buses is sufficient to carry out these studies. Using equation (2), we compute DC voltages for all lines and tabulate them in a vector \mathbf{V} .

Next, the GIC flow depends upon the real resistance of the various elements in the system and the path to the ground. As mentioned before, GICs are essentially DC; thus, the reactance of devices in the system is negligible for determining these currents. However, other resistances, like substation grounding resistance and transformer winding resistance, along with the configuration of transformers, come into play for computing the contribution of GICs.

For the purpose of computing GIC, we treat the three-phase transmission line and transformers (winding resistance) as being in parallel. Consequently, the total three-phase resistance is divided by three for each of the transformers and the transmission lines. These are in series with substation (or bus) grounding resistances. For example, for a transmission line between two substations, A and B, the total real resistance

is

$$R_{total}^{AB} = \sum_{tf} \frac{R_{tf,wind}^{3\phi}}{3} + \frac{R_l^{3\phi}}{3} + R_{ground}^A + R_{ground}^B \quad (3)$$

where $R_{tf,wind}^{3\phi}$ is the three-phase winding resistance for each of the transformers, $R_l^{3\phi}$ is the three-phase resistance for the transmission line, R_{ground}^A is the ground resistance for substation A, R_{ground}^B is the grounding resistance for substation B. Using equation (3), we generate the conductance matrix \mathbf{G} .

Lastly, using equation (1), we compute the DC currents flowing through the transmission lines, transformers, and other devices. Stacked currents are denoted by the vector \mathbf{I} . A standard convention for GIC analysis (Overbye et al. 2012) is to use the per-phase current for transformers and transmission lines. Thus, the GIC is computed per phase, i.e., $\mathbf{I}^{GIC} = \mathbf{I}/3$.

2.2 Transformer Failure Model under GIC

When quasi-DC GIC enters the winding through the neutral, it creates an additional flux that biases the operating point of the transformer, which severely reduces the efficiency of the transformer and causes heating. Therefore, we calculate the probability of failure as a function of the total current flowing through the transformer. Thus, the intensity of GIC and the current computed from the power flow study determines the total current, which forms the variable for the cascading failure probability analysis.

Transformers are manufactured with specific ratings, i.e., power, voltage, and current rating, along with margins in these for overloaded operation. If the current flowing through the transformer exceeds 20% over the rated current (typical margin) for that transformer, we consider that the transformer fails. This results in an incapacitated component and further overloading the remaining transformers. Re-running the power flow for the new system determines the current flowing through the rest of the transformers. Next, if the current flowing exceeds the rated current plus margin for another transformer among the remaining ones, then that transformer is said to have also failed. We continue removing transformers until the power flow calculation fails. This methodology provides a basis for assessing the risk of transformers dependent on the overload current and the intensity of geomagnetic storms quantified by GICs.

We suggest a linear relationship between the failure probability and the total current since the transformer fails due to overheating caused by the excess current flowing through it. The total current is the collective value from the GMD (\mathbf{I}^{GIC}) and the power flow solution. In this model, we choose normalized weights (adding up to 1) to define the failure probability distribution. These weights represent the importance of the outage current and the GIC in the failure model. For example, we can analyze cascading failures without the impact of GIC by setting $\alpha = 0$. Thus, the probability function for transformer i can be written as

$$P_f(TF_i) = \begin{cases} \alpha \left(\frac{I_i^{GIC}}{I_i^{max}} \right) + \beta \left(\frac{I_i^l}{I_i^{max}} \right), & \text{for } I_i^l, I_i^{GIC} \leq I_i^{max} \\ \alpha \left(\frac{I_i^{GIC}}{I_i^{max}} \right) + \beta, & \text{for } I_i^{GIC} \leq I_i^{max}, I_i^l > I_i^{max} \\ \alpha + \beta \left(\frac{I_i^l}{I_i^{max}} \right), & \text{for } I_i^{GIC} > I_i^{max}, I_i^l \leq I_i^{max} \\ 1 & \text{for } I_i^l, I_i^{GIC} > I_i^{max} \end{cases} \quad (4)$$

where $\alpha + \beta = 1$, I_i^{max} is the maximum rated current (a 20% margin on the rated value) for transformer i , I_i^l is computed by solving the power flow solution for the system with failed transformer(s), I_i^{GIC} is the GIC in transformer i as computed in Section 2.1.

For analysis and inference, we generate a table of probabilities associated with the transformers following a solar storm and the consequent removal of transformers from the system. Each row is associated with transformer $k = 1, \dots, N_{TF}$ (where N_{TF} is the total number of transformers in the system) while each column corresponds to an event. The first column is the occurrence of a solar storm. The following columns are the cascading events of incapacitating one transformer at a time. At each event, we turn off the transformer with the highest probability of failure. For example, the first column represents the initial failure probabilities of

Table 1: Generator Data.

Bus No.	Power Rating (MVA)	Voltage Rating (kV)	Assumed Config for GT
1 (Slack bus)	100	69	del-wye
2	100	69	del-wye
6	100	13.8	del-wye
3	100	69	del-wye
8	100	18	del-wye

Table 2: Transformer Data.

From Bus	To Bus	Assumed Configuration	Power rating (MVA)	Voltage rating (kV)
4	7	del-wye	100	69
4	9	del-wye	100	69
5	6	del-wye	100	69

Tables 1 and 2 show the generator and transformer data, i.e., the base ratings of power and voltages. Though the configuration of the transformers is not provided in the data, the transmission to distribution transformer has a typical configuration of delta-wye, and transmission system transformers are wye-wye connected. Note that the IEEE data do not model generator transformers (GT), and thus, for this example, we consider the ratings of these GTs to be the same as those of the generators to which they are attached. Furthermore, typically, the GTs have a configuration of delta-wye-to-ground connected, with the delta connection on the generator side. The rest of the bus and branch data for the power flow study of the IEEE 14-bus system can be found in (University of Washington 2014).

For the computation of the intensity of GIC, the resistance data for the components and ground resistance values for the buses (or substations) are also required. Unfortunately, these data are not part of the IEEE 14-bus test case, so we make the following assumptions.

1. The substation grounding resistance depends on several factors, including the size of the substations, for example, larger substations have a lower value, and also the resistivity of the ground; for example, rocky locations have higher values (Overbye et al. 2012). Typically, for most transmission and other larger substations, the ground resistance should be lower than 1Ω (IEEE Std 80 2015).
2. Typical transformer winding resistances generally range from a few milli-Ohms ($m\Omega$) to several Ohms (Ω), usually on the lower side. In power flow datasets, transformer impedance often does not include specific resistance values. In the absence of better information, estimation of resistance values may be made by standard values of X/R ratio for rated transformers given in (IEEE Std 242 2001). Furthermore, the individual coil winding resistances can be estimated as in (Overbye et al. 2012). For this probability modeling, in the absence of available data on winding resistances, we assume low resistance values based on the voltage rating of the transformers following (IEEE Std 389 2020).
3. GTs are not modeled separately and are sometimes included in generator data. For GTs, most resistance is on the high voltage side as the configuration is wye-grounded, and the delta on the low voltage side winding resistance can be ignored. Often the winding resistance of transformers is measured for given temperatures. In the absence of this data, we choose these values based on the size of the generator, i.e., their voltage rating following (IEEE Std 389 2020) for a fixed temperature value. Note that the temperature in the windings would increase as the current increases, changing the resistance values. However, in this probability modeling, we consider failure once a high current is reached in the transformer, and thus, disabling it, resulting in not using it in the subsequent probability computation.

Table 3: Failure probabilities for $I_i^{GIC} = 200A$ for all i .

$P_f(TF_i)$ with Transformer	No Disabled Transformer	1 Disabled Transformer	2 Disabled Transformers	3 Disabled Transformers	4 Disabled Transformers
TF 1 (bus 4 to bus 7)	0.2818	0.2911	0.3485	0.3558	-
TF 2 (bus 4 to bus 9)	0.2039	0.2092	0.2423	0.2479	0.5418 Power flow fails
TF 3 (bus 5 to bus 6)	0.3261	0.5126	-	-	-
TF 4 (GT at bus 1)	0.5996	-	-	-	-
TF 5 (GT at bus 2)	0.2798	0.1322	0.1026	0.1335	0.2038
TF 6 (GT at bus 6)	0.0697	0.3403	0.4404	0.2101	0.3272
TF 7 (GT at bus 3)	0.1967	0.0629	0.0567	0.0602	0.0682
TF 8 (GT at bus 8)	0.462	0.4377	0.5996	-	-

3.1 Failure Probability Computation for Chosen GIC Values

In this subsection, we consider a randomly chosen GIC value to simulate the probabilities of the failure of the transformers in the IEEE 14-bus system. This system has three transformers modeled in the line diagram (Figure 1) along with five other GTs for which we use the assumed rating of the generators they are attached. The ratings of all the transformers (and generators) are the same as in Tables 1 and 2.

We follow Algorithm 1 steps 5-9 to generate a probability table in this subsection. These steps are described in more detail below.

1. Run the power flow simulation. Compute the current flowing through all transformers for the given power flow solution. These calculations are in the per-unit system. Next, multiply the per-unit values by the base currents obtained from the voltage and power ratings to determine absolute values. This computation results in the current (I_i') flowing through each transformer i .
2. Compute the rated currents for the transformers and add a 20% margin to each resulting in the maximum current that the transformer can hold in overloaded conditions, I_i^{max} .
3. For the given values of GICs and computed currents, obtain the probability of failure of transformer i , i.e., $P_f(TF_i)$ from equation (4). In this example, we consider equal weights for the power flow current and GIC $\alpha = \beta = 0.5$. The computed probabilities are shown in the first column of Tables 3 and 4.
4. Pick the highest probability transformer (or the transformer that is the most likely to fail) and disable it from the system. Then, repeat steps 1-4 to compute the next set of probabilities. Continue these steps until power flow fails to converge or all GTs fail, failing the entire grid.

From Tables 3 and 4, the proportional relation between failure probability and intensity of GIC is distinctly observable. In general, with lower intensity of GIC circulating, the failure probabilities of transformers are lower than in the case of a stronger GIC value, as in Table 4.

In Table 3, following the most likely path of failures, we can compute the probability of failure of five transformers as a product of the highest probabilities at each event stage (each column), obtaining a value of 0.0355. Similarly, the probability of failure of four transformers is 0.0655, the probability of failure of three transformers is 0.184, and the probability of failure of two transformers is 0.307, i.e., for

Table 4: Failure probabilities for $I_i^{GIC} = 800A$ for all i .

$P_f(TF_i)$ with Transformer	No Disabled Transformer	1 Disabled Transformer	2 Disabled Transformers	3 Disabled Transformers	4 Disabled Transformers
TF 1 (bus 4 to bus 7)	0.5806	0.5899	0.6472	0.6545	-
TF 2 (bus 4 to bus 9)	0.5027	0.5080	0.5411	0.5467	0.8406 Power flow fails
TF 3 (bus 5 to bus 6)	0.6429	0.8113	-	-	-
TF 4 (GT at bus 1)	0.8984	-	-	-	-
TF 5 (GT at bus 2)	0.5786	0.4310	0.4014	0.4323	0.5026
TF 6 (GT at bus 6)	0.1294	0.4001	0.5001	0.2699	0.3870
TF 7 (GT at bus 3)	0.2747	0.1408	0.1346	0.1382	0.1462
TF 8 (GT at bus 8)	0.7607	0.7365	0.8984	-	-

transformer 4 (located at bus 1) and transformer 3 (located between buses 5 and 6), as shown in Table 3. These probabilities only represent one possible path of failure propagation after a solar storm based on the most likely event at each stage. We can compute probabilities of cascading failures for multiple paths similarly. For example, the probability of failure of transformer 4 located at bus 1 and failure of transformer 8 located at bus 8 is 0.262, and so on.

In Table 4, following the most likely to fail cascading path, the five transformers' failure probability is 0.36, while that of two transformers is 0.72. We observe that the overall probability of the most likely path of cascading failures is almost 10 times more for a higher GIC value of 800A (Table 4) than when the GIC intensity is 200A (Table 3).

In this subsection, we considered the same GIC flowing through each transformer. However, as mentioned in Section 2.1, the intensity of GIC depends on the geographical location and transformer configuration. In the following subsection, we compute GIC for two cases of electric field for arbitrarily chosen locations of the transformers and then perform the failure analysis.

3.2 Computation of GICs and Failure Probability for Given Electric Field

In this subsection, we implement the steps in Algorithm 1 to compute the failure probability table beginning with a notional solar storm. First, we compute the intensity of the GIC for a given electric field and the geographical coordinates of the buses following the steps in Section 2.1 for each transformer i . The ratings are given in Tables 1 and 2.

Once we compute the GIC values flowing through each transformer, we follow the steps in Algorithm 1 to compute the probabilities shown in Tables 5 and 6. As mentioned previously, the data for resistances required to determine the GIC values are not provided in the power system data, so we choose the values of these resistances according to IEEE standards and the typical values stated in Section 3.

For this test simulation, we arbitrarily assign geographic coordinates (in degrees) to the 14 buses of the IEEE-14 bus system. These coordinates are restricted to be within the US, and no two buses have a greater distance than 500 km or about 310 miles between them. The ground resistances are 0.1Ω for larger substations (or buses 1-5), 0.5Ω for buses 6-7,9-14, and 0.3Ω for bus 8. For probabilities computed

in Table 5, we choose $E = 1V/km$ electric field with an angle of $\theta = 90^\circ$ while for Table 6, we choose $E = 4V/km$ electric field with an angle of $\theta = 18^\circ$.

Table 5: Failure probabilities for $E = 1V/km$ with direction angle $\theta = 90^\circ$.

$P_f(TF_i)$ with Transformer	No Disabled Transformer	1 Disabled Transformer	2 Disabled Transformers	3 Disabled Transformers	4 Disabled Transformers
TF 1 (bus 4 to bus 7)	0.2086	0.1882	0.2392	0.2825	0.4413 Power flow fails
TF 2 (bus 4 to bus 9)	0.4365	0.4258	0.4553	0.4804	-
TF 3 (bus 5 to bus 6)	0.4202	0.4329	0.5920	-	-
TF 4 (GT at bus 1)	0.7809	0.7809	-	-	-
TF 5 (GT at bus 2)	0.3549	0.3777	0.2366	0.2086	0.2301
TF 6 (GT at bus 6)	0.0644	0.0966	0.2867	0.2048	0.2266
TF 7 (GT at bus 3)	0.5011	0.4907	0.3713	0.3646	0.3671
TF 8 (GT at bus 8)	0.8624	-	-	-	-

In both examples of this subsection (Tables 5 and 6), our model provides the initial probabilities of failure of a transformer when a solar storm occurs with a given value of electric field E in V/km along with cascading failure probabilities of the remaining transformers in the power system, which is also dependent on the overloading conditions due to the disabling of the transformers. We observe that this model is heavily dependent on the intensity of the solar storm, as can be seen from the probability values computed for the same GIC in Section 3.1 as well as location-specific GIC in this subsection. For example, the probabilities in Table 6 with $E = 4V/km$ are higher than those in Table 5 with $E = 1V/km$.

However, the dependency of the computed probabilities on the GIC is not straightforward in this subsection, as the intensity of GIC is different for different transformers. In most scenarios, as the number of failed transformers increases in the system, the failure probabilities of the remaining transformers increase. Nevertheless, this proportionality is not linear, as overloaded current values have a non-linear relationship with the power flow solution. Thus, as the failure cascades, some transformers could have a higher probability of failure than before while others may have the same or even slightly lower chances of failure, for example, GT at bus 3 in Table 6, has a lower probability of failure after removal of one transformer as compared to the initial probability (all transformers working).

In Table 5, the overall probability of the most likely path of cascading failure is 0.085, i.e., the probability of failure of five transformers. On the other hand, the overall probability of the most likely path of cascading failure is 0.22 in Table 6. These tables compare the path probabilities for the most likely cascading events. For comprehensive risk analysis, we can also compute and compare the probability of cascading failure paths for other combinations of failed transformers.

In Figure 2, we show average cascading failure probabilities for events corresponding to the number of failed transformers in the system. We generate 150 random values of the electric field E in the range of 1.5 V/km (Quebec event of 1982) and 20 V/km (Sweden event of 1921) (Kappenman 2010), with more values closer to the lower end, and random values of θ in radians. For each pair of (E, θ) , we use Algorithm 1 to obtain the probability tables. We follow the most likely failure path in that table to obtain cascading probabilities when one transformer fails, two transformers fail, and so on until power flow fails. We take

Table 6: Failure probabilities for $E = 4V/km$ with direction angle $\theta = 18^\circ$.

$P_f(TF_i)$ with Transformer	No Disabled Transformer	1 Disabled Transformer	2 Disabled Transformers	3 Disabled Transformers	4 Disabled Transformers
TF 1 (bus 4 to bus 7)	0.5298	0.5391	0.5585	0.6281	0.5146
TF 2 (bus 4 to bus 9)	0.2444	0.2497	0.2604	0.3025	0.2367
TF 3 (bus 5 to bus 6)	0.3447	0.5312	0.4498	0.4006	0.3995
TF 4 (GT at bus 1)	0.9857	-	-	-	-
TF 5 (GT at bus 2)	0.6802	0.5326	0.5718	0.6445	-
TF 6 (GT at bus 6)	0.5497	0.8204	-	-	-
TF 7 (GT at bus 3)	0.3067	0.1729	0.1760	0.1837	0.6360 Power flow fails
TF 8 (GT at bus 8)	0.5713	0.5471	0.6643	-	-

an average of the highest probability for each event in the 150 simulation runs to obtain the probability of failure of k transformers corresponding to the percentage of transformer failures ($p\%$) shown in Figure 2.

The histogram, in general, represents the probability of the proportion or percentage of transformers failing due to a solar storm. For example, an average probability that 37.5% transformers experience cascading failure is 0.586, or there is approximately a 60% chance that three (of the total eight) transformers fail due to a solar storm. Similarly, the chance of failure of 50% or half of the system transformers is approximately 44% in this 14-bus system.

While conducting this experiment, we also observed that if we consider more samples of the electric field intensity closer to 20 V/km, the probability of at least one transformer failing (or 12.5% of transformers failing) is very close to 1 and that of 25% of transformers failing is ≈ 0.85 implying that an intense solar storm can knock out two of the eight transformers of the IEEE 14-bus system with an 85% chance. Using the probability tables, one can also identify the two vulnerable transformers of this system that are more likely to fail for any given solar storm intensity.

4 CONCLUSION AND FUTURE WORK

The proposed model's validation requires past data comparisons, which are rare due to the low frequency of such events. The existing solar storm simulators generate GMDs and model specific physical properties of the transformers but not their impacts on the grid's reliability. In fact, to the best of our knowledge, no commercially available simulators assess the chance of failure of power grid transformers directly following a solar storm. Future validation of the model will require comparing it with one of the rare events like the Quebec blackout in 1989. The next step in our approach is to investigate the data availability for the transformers of the Quebec power grid. For instance, the transformer configuration is required to assess the intensity of GICs. In the simplest case of a grounded wye-delta, such as in GTs, I^{GIC} is just the current in the grounded coil as computed, while for autotransformers it depends on the turns ratio as well. Also, the wye connection of the transformer is vulnerable to GICs due to the path to the ground, unlike the delta connection. Other factors, such as ground impedances, are also necessary to carry out a practical study. Collecting these data for systems of interest will be an important step toward a practical tool for risk assessment.

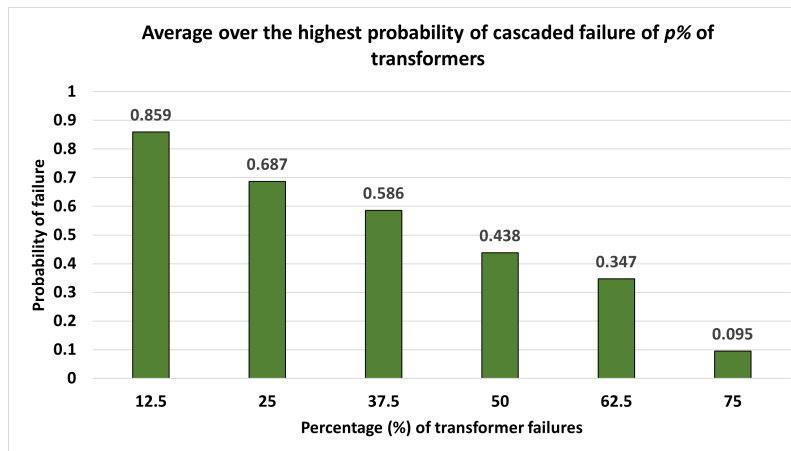


Figure 2: Average of the highest probabilities for k cascaded transformer failures over 150 randomly chosen electric field intensity values $((E, \theta))$.

A standard definition of risk is the product of likelihood and cost. Therefore, one of the next steps in the development of the model is to include economic and societal losses associated with transformer failures. Indeed, these losses may be severe, and their likelihoods warrant careful study. In a vivid description of the possible aftermath of an exceptionally powerful solar storm, (Kappenman 2012) states that –“*of all the parts of the power grid, high-voltage transformers are among the most likely to fail in a geomagnetic storm and also among the most difficult to replace. ... EHV transformers, which can handle voltages of 345 kV or higher, weigh about 200 tons and cost about \$10 million each. Building one requires exquisite, near-artisanal craftsmanship, including meticulously hand-winding the paper-tape insulation around the copper winding at the transformer’s core. ... Even the largest transformer plants can build only about 30 to 50 per year.*” In particular, the risk associated with failing transformers can result in an evaluation criterion for “switching off” transformers to interrupt the flow of GIC and result in a possible strategy for reducing collective losses.

The challenging societal consequences of a prolonged blackout resulting from a considerable loss of these difficult-to-replace transformers warrant careful future consideration. The costs of these consequences, tempered by an understanding of the likelihood of their occurring, will play an important role in ensuring the resilience of our electrical power systems.

ACKNOWLEDGMENTS

This manuscript has been authored by UT-Battelle, LLC under Contract No. DE-AC05-00OR22725 with the U.S. Department of Energy, Office of Science, Advanced Scientific Computing Research (ASCR) program. The United States Government retains and the publisher, by accepting the article for publication, acknowledges that the United States Government retains a non-exclusive, paid-up, irrevocable, worldwide license to publish or reproduce the published form of this manuscript or allow others to do so, for United States Government purposes. The Department of Energy will provide public access to these results of federally sponsored research in accordance with the DOE Public Access Plan (<http://energy.gov/downloads/doe-public-access-plan>).

REFERENCES

- IEEE Std 242 2001. “IEEE Recommended Practice for Protection and Coordination of Industrial and Commercial Power Systems (IEEE Buff Book)”. <https://ieeexplore.ieee.org/document/974402>, accessed 20.03.2023.
- IEEE Std 389 2020. “IEEE Recommended Practice for Testing Transformers and Inductors for Electronics Applications”. <https://ieeexplore.ieee.org/document/9084213>, accessed 20.03.2023.

- IEEE Std 80 2015. "IEEE Guide for Safety in AC Substation Grounding". <https://ieeexplore.ieee.org/document/7109078>, accessed 20.03.2023.
- Albertson, V., J. Kappenman, N. Mohan, and G. Skarbakka. 1981. "Load-flow Studies in the Presence of Geomagnetically Induced Currents". *IEEE Transactions on Power Apparatus and Systems* (2):594–607.
- Boteler, D., and R. Pirjola. 1998. "Modelling Geomagnetically Induced Currents Produced by Realistic and Uniform Electric Fields". *IEEE Transactions on Power Delivery* 13(4):1303–1308.
- Boteler, D. H. 2019. "A 21st-Century View of the March 1989 Magnetic Storm". *Space Weather* 17(10):1427–1441.
- National Research Council 2009. "Severe Space Weather Events Understanding, Societal and Economic Impacts: A Workshop Report: Extended Summary".
- Dehghanian, P., K. S. Shetye, K. R. Davis, and T. J. Overbye. 2019. "System-wide Case Study Assessment of Transformer Heating Due to Geomagnetic Disturbances". In *2019 North American Power Symposium (NAPS)*, 1–6. IEEE.
- Force, NERC Geomagnetic Disturbance Task 2012. "Special Reliability Assessment Interim Report: Effects of Geomagnetic Disturbances on the Bulk Power System".
- Hayakawa, H., Y. Ebihara, D. M. Willis, S. Toriumi, T. Iju, K. Hattori, M. N. Wild, D. M. Oliveira, I. Ermolli, J. R. Ribeiro, A. P. Correia, A. I. Ribeiro, and D. J. Knipp. 2019. "Temporal and Spatial Evolutions of a Large Sunspot Group and Great Auroral Storms Around the Carrington Event in 1859". *Space Weather* 17(11):1553–1569.
- Kappenman, J. 2010. *Geomagnetic Storms and Their Impacts on the US Power Grid*. Citeseer.
- Kappenman, J. 2012. "A Perfect Storm of Planetary Proportions". *IEEE Spectrum* 49(2):26–31.
- Lloyd's 2013. "Solar Storm Risk to the North American Electric Grid". <https://www.lloyds.com/news-and-insights/risk-reports/library/solar-storm>, accessed 12.04.2023.
- Department of Energy 2019, July. "North American Energy Resilience Model". <https://www.energy.gov/oe/articles/north-american-energy-resilience-model-july-2019>, accessed 12.04.2023.
- University of Washington 1993. "Power Systems Test Case Archive". http://labs.ece.uw.edu/pstca/pf14/pg_tca14bus.htm, accessed 20.03.2023.
- University of Washington 2014. "IEEE 14-Bus System Description". <https://matpower.org/docs/ref/matpower5.0/case14.html>, accessed 20.03.2023.
- Overbye, T. J., T. R. Hutchins, K. Shetye, J. Weber, and S. Dahman. 2012. "Integration of Geomagnetic Disturbance Modeling into the Power Flow: A Methodology for Large-scale System Studies". In *2012 North American Power Symposium (NAPS)*, 1–7. IEEE.
- Ramírez-Niño, J., C. Haro-Hernández, J. H. Rodríguez-Rodríguez, and R. Mijarez. 2016. "Core Saturation Effects of Geomagnetic Induced Currents in Power Transformers". *Journal of Applied Research and Technology* 14(2):87–92.
- Texas A&M University 2016. "Electrical Grid Test Case Repository". <https://electricgrids.engr.tamu.edu/electric-grid-test-cases/ieee-14-bus-system/>, accessed 20.03.2023.

AUTHOR BIOGRAPHIES

PRATISHTHA SHUKLA is a Postdoctoral Research Associate in the Computational Systems Engineering & Cybernetics Group at Oak Ridge National Laboratory. She graduated from North Carolina State University with a Ph.D. in Electrical Engineering in 2021 where her area of study was game-theoretic methods for cyber-security in networked control systems with applications to large-scale power systems. Her current research interests include optimization, game theory, stochastic modeling, and energy systems. Her email address is shuklap@ornl.gov.

JAMES NUTARO is Group Lead for the Computational Systems Engineering & Cybernetics Group at Oak Ridge National Laboratory. He holds a Ph.D. in Computer Engineering from the University of Arizona. His research interests discrete event systems, systems modeling and simulation, and hybrid dynamic systems. His email address is nutarojj@ornl.gov.

SRIKANTH YOGINATH is a senior research staff member in the Computer Science and Mathematics division of the Oak Ridge National Laboratory, Oak Ridge, TN. Dr. Yoginath obtained his PhD in Computational Sciences and Engineering from Georgia Institute of Technology in 2014. His research areas include large-scale parallel and distributed computing, modeling and simulations, and machine learning. His email address is yoginathsb@ornl.gov.